



Domains and Rafts in Membranes – Hidden Dimensions of Selforganization

R. LIPOWSKY

Max-Planck-Institute of Colloids and Interfaces, 14424 Potsdam, Germany

Abstract. Both biomembranes and biomimetic membranes such as lipid bilayers with several components contain intramembrane domains and rafts. Macromolecules, which are anchored to the membrane but have no tendency to cluster, induce curved nanodomains. Clustering of membrane components leads to larger domains which can grow up to a certain maximal size and then undergo a budding process. The maximal domain size depends on the interplay of spontaneous curvature, bending rigidity, and line tension. It is argued that this interplay governs the formation of both clathrin-coated buds and caveolae. Finally, membrane adhesion often leads to domain formation within the contact zone.

Key words: adhesion, anchored polymer, anchored sticker, budding, caveolae, curvature, domain, membrane, raft

1. Introduction

The amazing architecture of biological systems is based, to a large extent, on the spatial organization of biomembranes which involves a wide range of length scales. On the nanometer scale, these membranes consist of lipid bilayers which provide an interface for the anchoring of many types of proteins and polysaccharides. A simplistic cartoon of this supramolecular structure is shown in Figure 1.

On the micrometer scale, biomembranes represent highly flexible surfaces which partition space into nested compartments and undergo unusual shape transformations such as budding. The latter process consists in the formation of small, spherical buds which are expelled from a larger membrane segment. In biological cells, budding is an ubiquitous process and represents the first step in the production of vesicles for transport through cell membranes and between different intracellular compartments.

It is quite remarkable that such a budding process, which may be observed in the light microscope, directly implies that the membrane has a certain type of molecular organization. Indeed, both the membrane forming the bud and the surrounding membrane matrix must be in a *fluid* state in which the molecules can flow and rearrange themselves within the plane of the membrane.

A typical biomembrane contains a large number of different lipids, proteins and polysaccharides, some of which are indicated in Figure 1. For a fluid membrane,

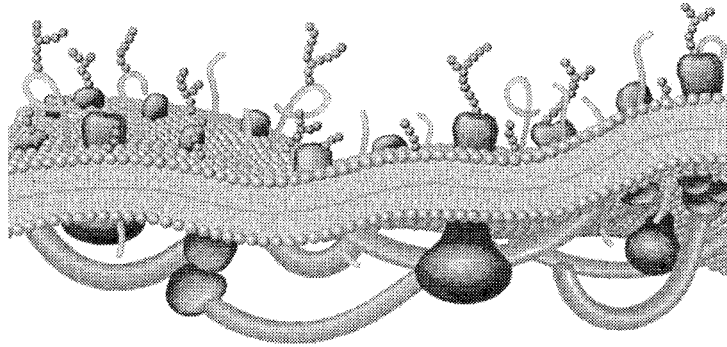


Figure 1. Cartoon of biomembrane which consists of a lipid bilayer with many anchored components.

these different components undergo rapid lateral diffusion within the membrane. Thus, a single lipid molecule usually explores a membrane area of about $1 \mu\text{m}^2$ in one second provided the membrane has a uniform composition.

It is intuitively clear that the different membrane components will interact in various ways. If some components have a tendency to cluster, they may form intramembrane domains with specific properties. A priori, one would expect that these domains can become as large as the membrane itself. It turns out, however, that fluid domains in fluid membranes *can only grow up to a certain maximal size* which depends on the membrane composition [1, 2, 3]. As soon as they reach this maximal size, the domains spontaneously form buds. This process of domain-induced budding provides a simple and generic mechanism and has presumably been observed for several biomimetic membranes [4, 5, 6].

It has been known for a long time that biomembranes also contain intramembrane domains even though there has been some controversy about the relative importance of lipids and proteins in these structures. Budding of the plasma membrane often involves domains which are covered by a network of coat proteins such as clathrin; for a recent review, see [7]. Likewise, the formation of caveolae, which are cave-like invaginations of the plasma membrane, seems to require the protein caveolin. However, it is now widely believed that caveolae are formed from certain lipid domains or rafts containing glycosphingolipids and cholesterol [8, 9, 10]. It had been argued for some time that cell membranes contain domains which are enriched in glycosphingolipids [11] or cholesterol [12]. The raft concept promotes the idea that these two types of molecules work together in order to fulfill a variety of biological functions. Indeed, rafts and caveolae provide an important pathway for signalling and endocytosis, the latter being sometimes misused by 'smart' viruses [13, 14].

From the physical point of view, the simplest way to initiate domain formation in a multicomponent system is to quench it into a two-phase coexistence region

and to nucleate domains of the minority phase within the majority phase. Fluid-fluid coexistence has been frequently observed in lipid *monolayers* at the air-water interface. One example is provided by monolayers prepared from the plasma membrane of red blood cells which contains a mixture of different lipids and cholesterol [15].

For *bilayer* membranes containing similar components, several types of experiments gave some evidence for an analogous fluid-fluid coexistence but it was not possible, for many years, to directly observe the corresponding membrane domains. Very recently, this has been achieved for multicomponent bilayers containing a mixture of DOPC, cholesterol, and spingomyelin [16] using improved methods of optical microscopy [17, 18].

In this article, I will briefly review some of our theoretical work on domains in membranes. First, in Section 2, membranes are decorated with anchored molecules which protrude from the membrane but have no tendency to form clusters. These molecules exert a local pressure onto the membrane and, in this way, lead to curved nanodomains. In addition, the anchored molecules undergo thermal collisions which make another contribution to the membrane curvature. In Section 3, some of the membrane components mutually attract each other and, thus, form intramembrane domains which are large compared to the size of a single molecule. These domains can only grow up to a certain maximal size which depends on their composition and, thus, on their bending rigidity, spontaneous curvature and line tension. Finally, Section 4 contains a brief discussion of adhesion-induced domain formation. In all cases, possible implications for the behavior of biomembranes are emphasized.

2. Anchored Molecules and Curvature

First, let us consider a bilayer membrane with some anchored macromolecules. Thus, the membrane contains one or several lipid components and, in addition, one macromolecular component which is large compared to the lipids and protrudes from the bilayer membrane. These macromolecules may be polysaccharides or proteins which are covalently attached to the head groups of some lipids or they may be anchored by a hydrophobic segment spanning the whole bilayer. In addition, one can construct synthetic polymers which have one or several hydrophobic anchors, see Figure 2.

The synthetic polymers shown in Figure 2 are usually chainlike molecules built up from a single monomer. In order to attach such a homopolymer to the membrane surface, the polymer must be soluble in water (otherwise, it would prefer to sit inside the membrane). On the other hand, biopolymers such as proteins or RNA are built up from different types of monomers. These molecules usually fold into more or less compact objects, the surface of which is covered by the more hydrophilic monomers. In the following, the term ‘polymer’ is used both for synthetic and for biopolymers.

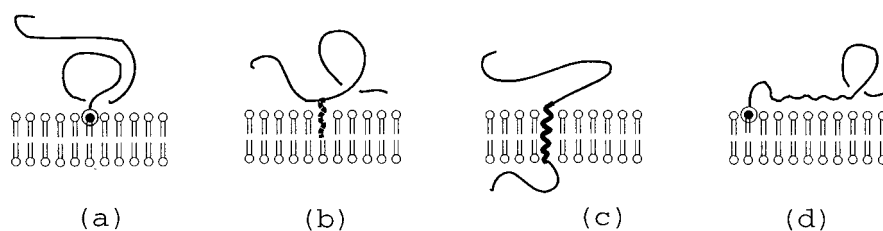


Figure 2. Polymers attached to bilayer membranes: (a)–(c) *Anchored coils* and (d) *Adsorbed coil* for which the nonanchored part is *repelled* from and *attracted* towards the membrane, respectively.

The simplest membrane composition corresponds to a small concentration of polymers which are soluble in water and have no tendency to form clusters or aggregates. The conformation of such a polymer depends on the membrane polymer interactions: If the nonanchored part of the polymer is repelled from the membrane surface, it forms an *anchored coil*; if this part is attracted to the membrane, it forms an *adsorbed coil*, see Figure 2. In polymer physics, ‘anchored coils’ and ‘adsorbed coils’ are often called ‘mushrooms’ and ‘pancakes’. I will avoid this terminology here since both cases look like ‘mushrooms’ in the presence of a membrane anchor.

Anchored and/or adsorbed coils exert spatially varying pressures onto the membrane and, thus, act to curve the membrane locally [19–23]. The sign and magnitude of this induced curvature reflects the entropic and enthalpic contributions to the polymer-membrane interactions. In addition, the lateral diffusion of the anchored molecules leads to collisions between them which also contribute to the membrane curvature. These two effects are described in the next two subsections.

Biomimetic membranes containing anchored polymers have also been studied by a variety of experimental methods [24–31]. In all of these studies, the anchored polymers were observed to have a strong effect on the shape of the membranes.

2.1. CURVATURE INDUCED BY SINGLE MOLECULES

From the physical point of view, the simplest macromolecule is a linear homopolymer, i.e., a linear chain of identical monomers. Its properties are essentially controlled by three parameters: the solvent quality, the chain length measured by the monomer number, N , and the polymer concentration. In the absence of external constraints or forces, such a polymer forms a free coil which has the linear size $R_{po} \sim a_{po}N^\nu$ with the size exponent ν and the persistence length a_{po} . The size exponent is $\nu \simeq 3/5$ for good solvents and $\nu = 1/2$ for θ -solvents corresponding to ideal chains.

Now, consider such a polymer which is anchored to the membrane via a certain anchor segment. This anchor segment may be located at the end of the linear chain as in Figure 2(a), it may correspond to a hydrophobic sidegroup as in Figure 2(b),

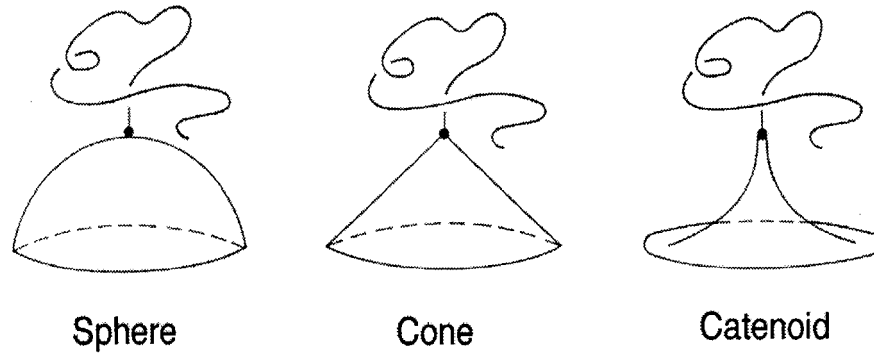


Figure 3. Anchored coils at membrane segments of different shapes which reflect the entropic repulsion between the polymer and the membrane.

or it may be a membrane spanning segment as in Figure 2(c). For the three cases displayed in Figure 2(a)–(c), the nonanchored part of the polymer is repelled from the membrane and, thus, forms an anchored coil. On the other hand, a polymer, which is attracted to the membrane, forms an adsorbed coil with many contact points as in Figure 2(d). One example for the latter situation is provided by a negatively charged polymer anchored to a positively charged membrane.

For simplicity, the bilayer membranes in Figure 2 have been drawn as flat sheets. However, since the anchored and adsorbed coils are in direct contact with the membrane, they exert forces and bending moments onto the adjacent membrane segment.

Anchored coils

The curvature induced by anchored coils (or ‘mushrooms’) has been determined theoretically using scaling arguments, analytical calculations for ideal chains, and Monte Carlo simulations [19–21]. As a result, one finds that the membrane always bends away from the polymer as shown in Figure 3. In addition, the magnitude of this local curvature has universal features: it is given by [19]

$$M_{sp} \sim T/\kappa R_{po} \sim T/\kappa a_{po} N^{\nu} \quad \text{for anchored coils} \quad (1)$$

and, thus, only depends on the linear polymer size R_{po} and on the ratio of the bending rigidity κ and the temperature T (measured in energy units).

Using the systematic methods of statistical field theory, one can also calculate the spatially dependent local pressure, which the polymer exerts onto the membrane, as well as the average shape of the curved membrane [21]. As a result, the membrane is found to have a cone-like shape close to the anchor segment and to attain a catenoid-like shape further away from it, compare Figure 3.

One may also determine the curvature arising from an ensemble of \mathcal{N} polymer coils which are anchored on one side of a membrane with area \mathcal{A} . Each anchored

coil affects the adjacent membrane segment with area \mathcal{A}_1 where it induces the spontaneous mean curvature M_{sp} as given by (1). Averaging over the total area \mathcal{A} of the membrane, one then obtains the spontaneous mean curvature $\bar{M}_{sp} \cong M_{sp} \mathcal{N} \mathcal{A}_1 / \mathcal{A}$ or [21]

$$\bar{M}_{sp} = c_1 \frac{T}{\kappa} R_{po} \frac{\mathcal{N}}{\mathcal{A}} \quad \text{with} \quad c_1 \cong \frac{1}{4} \left(\frac{\pi}{6} \right)^{1/2} \simeq 0.18. \quad (2)$$

The anchored coil also increases the bending rigidity κ of the membrane segment by $\Delta\kappa = c_\kappa T$ [20]. Recent experiments on ternary microemulsions give strong evidence for this effect and lead to the estimate $c_\kappa \simeq 1.5$ [30].

Coils anchored at both ends

If the polymer chain is anchored at *both* ends, one has two competing effects. When the two ends are close together, the polymer forms an anchored ring and the membrane again bends away from the chain. On the other hand, if both ends are far apart, the polymer is in a stretched state and then pulls on the membrane. For ideal chains with $\nu = 1/2$, these two competing effects cancel to leading order and the polymer-induced curvature vanishes [32].

Adsorbed coils

For adsorbed coils (or ‘pancakes’), the membrane has a tendency to bend towards the polymer in order to increase the number of contact points but it may also bend away from the polymer depending on the details of the polymer-membrane interactions [22, 23]. In fact, the sign and magnitude of the polymer-induced curvature is found to depend on several molecular length scales such as the range of the polymer-membrane interaction potential and the size of the anchor segment [23].

2.2. CURVATURE INDUCED BY MOLECULAR COLLISIONS

The polymer-induced curvature discussed so far arises from the entropic and enthalpic interactions between the anchored molecules and the membrane. Since the membrane is fluid, these molecules diffuse and occasionally collide. These collisions between the anchored macromolecules give another contribution to the membrane curvature as explained next.

Consider again a membrane segment of area \mathcal{A} with \mathcal{N} molecules anchored on one side of the membrane. These molecules can have various shapes as indicated in Figure 4. The ball shape, for instance, may correspond to the average shape of a water-soluble polymer coil as discussed before or it may describe the compact shape of an anchored protein. Each molecular shape shown in Figure 4 is characterized by two length scales, R and ℓ . The length scale R corresponds to the radius of the largest cross-section parallel to the membrane surface. The length scale ℓ measures the distance of this cross-section from the midplane of the bilayer membrane; thus, the distance ℓ is at least half the bilayer thickness.

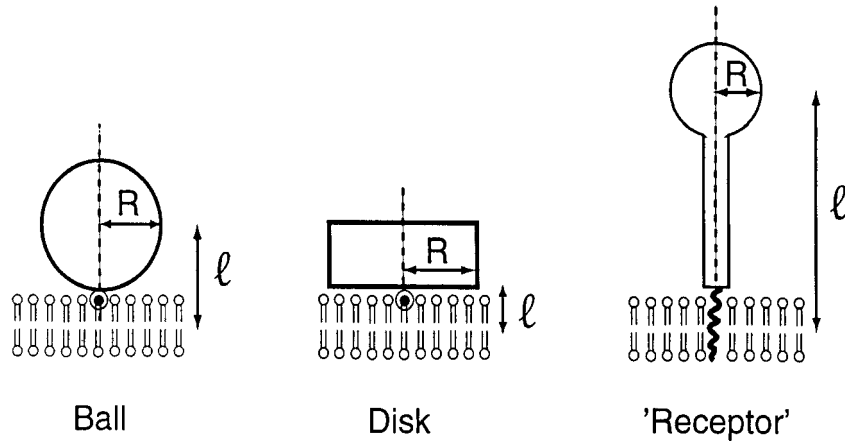


Figure 4. Macromolecules of different shapes anchored to bilayers. The length scale R corresponds to the radius of the largest cross-section parallel to the membrane surface. The length scale ℓ measures the distance of this cross-section from the midplane of the bilayer membrane.

In the planar membrane state, the anchored molecules behave as a two-dimensional gas of particles with hard core radius R . If the membrane has mean curvature M , the hard core radius is effectively reduced and becomes $R_{\text{eff}} \approx R(1 - \ell M)$. Therefore, the membrane bends away from the anchored molecules and attains the spontaneous mean curvature

$$\bar{M}_{sp} \approx \pi \frac{T}{\kappa} \ell R^2 \left(\frac{\mathcal{N}}{\mathcal{A}} \right)^2 \quad (3)$$

as follows from a virial expansion of the free energies. It is interesting to note that this effect arising from the collisions between the anchored molecules is already important in the low coverage regime, long before the molecules become closely packed on the membrane.

2.3. IMPLICATIONS FOR BIOMEMBRANES

Membrane proteins are believed to be rather rigid. Possible exceptions are provided by the loop segments between two membrane spanning segments. However, a flexible loop segment, which is anchored at both of its ends, does not induce any membrane curvature if it behaves like an ideal chain, see Section 2.1 above. In fact, the only segments of an ideal chain, which act to bend the membrane, are the first and the last segment which have only one anchor point [32]. Likewise, a protruding receptor as shown in Figure 4 may be too rigid to make additional contacts with the membrane surface. In principle, the size and the shape of the anchor segment may induce some curvature [19] but this effect is difficult to estimate in general since smaller membrane molecules such as cholesterol frequently undergo flip flops

between the two monolayers which tends to relax local elastic strains within the bilayer.

On the other hand, membrane proteins, which diffuse laterally in the membrane, should bend the bilayer membrane via mutual collisions and, thus, induce the mean curvature as given by (3). This mechanism may be relevant for lipid rafts. Indeed, it has been recently argued that lipid rafts recruit certain membrane proteins and receptors. If \mathcal{N} such receptors, characterized by the two length scales R and ℓ as in Figure 4, are anchored on the same side of the raft domain with area \mathcal{A} , this domain should acquire the spontaneous mean curvature $\bar{M}_{sp} \sim \ell R^2 (\mathcal{N}/\mathcal{A})^2$.

3. Domain-Induced Budding of Membranes

In the previous section, we considered a multicomponent membrane for which none of its components had a tendency to form clusters or aggregates. Now, let us assume that some of these components mutually attract each other and form intramembrane domains which are large compared to the size of a single molecule.

3.1. BUDDING OF A SINGLE DOMAIN

First, consider a single membrane domain, say β , which has been nucleated within a membrane matrix, say α , and which now grows by diffusion-limited aggregation as shown in Figure 5. By definition, an intramembrane domain has a composition which differs from the composition of the membrane matrix. This difference in composition will usually lead to a difference in spontaneous curvature. In addition, the boundary of the domain gives a free energy contribution which is proportional to its length. The corresponding free energy density defines the line tension λ . In general, both the spontaneous curvature and the line tension provide a driving force for budding [1].

Even for vanishing spontaneous curvature, a *flat* domain of linear size L does not necessarily represent the state of lowest free energy since the length of the domain boundary can be reduced if the domain forms a bud: the domain boundary now forms the neck of the bud, and this neck narrows down during the budding process, see Figure 5. Since the bud is curved, its formation will cost some bending free energy. However, since the free energy of the domain boundary is proportional to the domain size L whereas the bending free energy of the bud does not depend on the bud size (for $M_{sp} = 0$), the domain *must* bud as soon as its size L exceeds a certain maximal size L_{\max} [1]. This is true in general provided the membrane is not under lateral tension as will be assumed here.

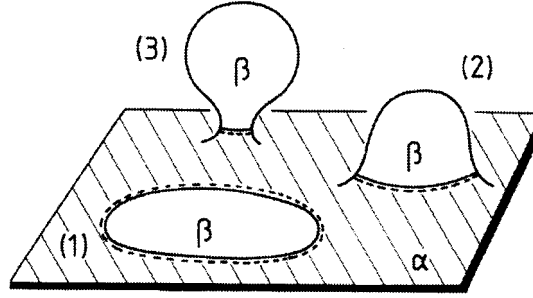


Figure 5. A fluid domain (β) in a fluid matrix (α) undergoes a budding transformation as soon as the domain size has reached a certain maximal value, which depends on the interplay of spontaneous curvature, bending rigidity, and line tension. The successive stages of the budding process are indicated by (1), (2) and (3).

Maximal domain size

If one ignores the curvature of the α matrix, the maximal size L_{\max} of the β domain depends on its spontaneous mean curvature M_{sp} and on the length scale $\xi \cong \kappa/\lambda$. This maximal size has the general form [1]

$$L_{\max} = L_{\max}(\xi, M_{sp}) = \xi \Omega(\xi | M_{sp}) \quad (4)$$

where the function $\Omega(x)$ decreases monotonically with increasing $x \equiv \xi M_{sp}$. Therefore, one has $L_{\max}(\xi, M_{sp}) \leq \xi \Omega_0$ with $\Omega_0 \equiv \Omega(0)$. The simple model studied in [1], which ignores the precise shape of the neck region, leads to $\Omega_0 = 8$. One may also use the results obtained for limit shapes of vesicles with two domains [2] and consider the limiting case in which the bud is small compared to the total vesicle. The corresponding neck condition then leads to $\Omega_0 = 4$ as explained further below.

For a lipid bilayer, the bending rigidity has the typical value $\kappa \simeq 10^{-19}$ J. In order to estimate the line tension λ , we may consider two adjacent domains consisting of two different types of lipids, say A and B . The interaction energies for pairs of AA , BB , and AB lipids are denoted by U_{AA} , U_{BB} , and U_{AB} , respectively. A simple estimate for the line tension of the domain boundary within one monolayer is then given by $\lambda \simeq \Delta E/a$ with the energy difference $\Delta E \cong [\frac{1}{2}(U_{AA} + U_{BB}) - U_{AB}]$ where $a \simeq 0.8$ nm is the lateral dimension of the lipids. Depending on the architecture of the lipids, the main contribution to this energy difference may come from the head groups of the lipids, from the different backbones of glycerolipids and sphingolipids, or from saturated versus unsaturated acyl chains, but should be of the order of $k_B T \simeq 4.1 \times 10^{-21}$ J. This implies the estimate $\lambda \simeq 2k_B T/a \simeq 10^{-11}$ N where the factor 2 reflects the two monolayers of the bilayer. Finally, the values $\kappa \simeq 10^{-19}$ J and $\lambda \simeq 10^{-11}$ N lead to a maximal domain radius $L_{\max}(\xi, 0)$ of about 80 nm [1].

The addition of 30 percent cholesterol increases the bending rigidity of DMPC bilayers by about a factor of four [33]. Monolayers containing this mixture are close to a critical point at which the line tension vanishes; for zero lateral pressure, the corresponding line tension has been measured to be about 2×10^{-12} N [34]. This implies that, for bilayers containing 70 percent DMPC and 30 percent cholesterol, the maximal domain radius $L_{\max}(\xi, 0)$ should be about 800 nm.

Neck condition for complete buds

A vesicle which consists of two domains α and β often attains a limit shape in which the β domain forms a complete bud, i.e., a spherical bud which is connected to the mother vesicle by an infinitesimal neck. The domain boundary is contained in this neck. Adjacent to the neck region, the mean curvature M^β of the bud and the mean curvature M^α of the mother vesicle satisfy the condition [2]

$$\kappa^\alpha (M^\alpha - M_{sp}^\alpha) + \kappa^\beta (M^\beta - M_{sp}^\beta) = \lambda/2 \quad (5)$$

where the bending rigidities κ^α and κ^β , and the spontaneous mean curvatures M_{sp}^α and M_{sp}^β of the α and β domains will, in general, be different. If the first term on the left hand side of (5) is small, this condition becomes equivalent to $1/M^\beta = 2\xi/(1 + 2\xi M_{sp}^\beta)$ which is a special case of (4).

3.2. BUDDING OF MANY DOMAINS

The phase separation process within a multicomponent membrane will usually lead to the formation of many intramembrane domains. As long as the lateral tension within the membrane is small, the membrane will form many small buds. The simplest situation corresponds to a membrane with two components, say A and B , as shown in Figure 6. This figure displays a sequence of vesicle shapes as observed in Monte Carlo simulations. The vesicle membrane consists of two different types of triangles or patches. For the example shown in Figure 6, one has 1200 bright and 1200 dark patches with zero and positive spontaneous curvature, respectively [3].

Each membrane patch should be regarded as a small, preassembled cluster of membrane molecules. The size of these patches is about 6 nm which is comparable to the smallest wavelength of bending modes [35]. Therefore, the total area of the membrane shown in Figure 6 is about 2400×36 nm² which corresponds to a relatively small vesicle with a radius of about 80 nm. At present, larger vesicles are not accessible to Monte Carlo (or any other type of computer) simulations.

Since the simulated vesicles are rather small, the volume of these vesicles was allowed to adapt freely in order to ensure that the vesicle membrane stayed tensionless during the budding process. One then obtains a relatively high surface density of buds as shown in Figure 6. In real systems, the membrane may be subject to various constraints which can induce a lateral tension and, in this way, decrease the surface density of buds [1].

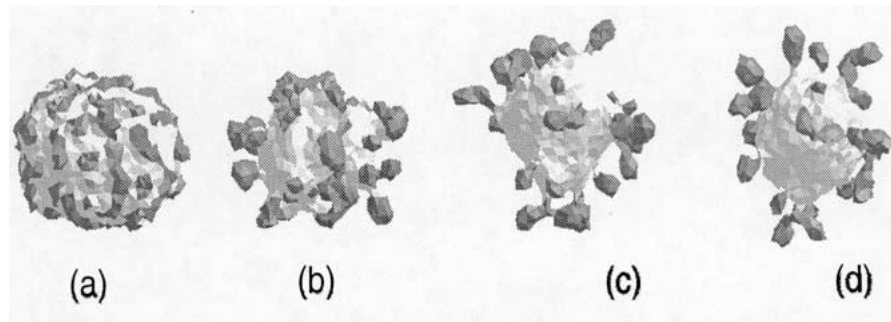


Figure 6. Shape sequence of a two-component membrane as observed in Monte Carlo simulations. The bright and dark patches have zero and finite spontaneous curvature, respectively. (a) Formation and growth of domains; (b), (c) Formation of many buds ; and (d) Coalescence of small buds into larger ones. The membranes shown here are tensionless. A lateral tension will reduce the surface density of buds, see text.

Inspection of Figure 6 shows that the formation of many buds involves three distinct time regimes: [3] (i) Formation and growth of intramembrane domains; (ii) Multiple bud formation; and (iii) Coalescence of small buds into larger ones. If the domains forming the bud have a spontaneous curvature, the buds become more tubelike as they grow in size. Time regime (i) corresponds to the usual phase separation dynamics in two-dimensional systems. The time regimes (ii) and (iii) are unique to flexible membranes and reflect their ability to escape into the third dimension.

3.3. IMPLICATIONS FOR BIOMEMBRANES

As mentioned before, a smooth budding process implies that both the membrane forming the bud and the surrounding membrane matrix must be in a fluid state in which the molecules can flow and rearrange themselves. Indeed, the compressibility of bilayer membranes is rather small and its area can only be changed by a few percent before the membranes become leaky and start to rupture. If such a membrane were in a solid-like or polymerized state, in which the molecules have a fixed spatial position, the smooth formation of a spherical bud would be impossible as one can easily demonstrate with a sheet of paper. As an alternative to a smooth budding process, one could envisage an active cut and paste procedure [1] but this would require a rather complex molecular machinery.

Clathrin-coated domains

Endocytosis is a frequent budding event of the plasma membrane by which the cell takes up macromolecules and other large particles from the extracellular fluid. The first pathway for endocytosis, which was studied in some detail, involves clathrin-coated domains. The elementary building blocks of the coat are receptor

molecules with clathrin trimers (or triskelions) attached to receptor tails via assembly polypeptides. In vitro, these trimers spontaneously assemble into polyhedral cages which have a radius between 40 and 60 nm. Because of this self-assembly process, it is often argued that the polymerization of the clathrin network drives the budding process, see, e.g., [7].

It is not possible to observe the time evolution of the budding process of clathrin-coated domains directly since the domains are too small. However, electron micrographs show various intermediate states of this process and, thus, strongly indicate that it proceeds in a smooth way. This seems to imply that the clathrin polymerization represents the final step after budding has essentially been completed [1]. In this view, the budding is primarily driven by the interplay of spontaneous curvature, bending rigidity and line tension as described in Section 3. These parameters are, however, affected by the adsorption of the coat molecules.

Obviously, the adsorption of a coat protein on one side of the membrane changes its asymmetry and, thus, its spontaneous curvature. One contribution to this curvature arises from the collision mechanism, described in Section 2.2, as long as the receptor molecules which bind the clathrin are still laterally mobile. In addition, both the bending rigidity κ and the line tension λ are expected to increase with the adsorption of the coat. As discussed in Section 3.1, the maximal domain size L_{\max} is determined by the spontaneous curvature M_{sp} and the length scale $\xi = \kappa/\lambda$. This maximal domain size changes from its initial value L_{\max}^i before the adsorption of coat protein to its final value L_{\max}^f after this adsorption. Thus, if the maximal domain size is reduced by the coat adsorption, all domains, which have a size L with $L_{\max}^f < L < L_{\max}^i$, will undergo a budding process.

Caveolae and lipid rafts

Caveolae are cave-like invaginations of the plasma membrane with a diameter of 50–100 nm. It has been recently proposed that these caveolae are formed from flat lipid domains or rafts consisting of glycosphingolipids, cholesterol and various colocalized proteins [8–10]. In vivo, the formation of caveolae seems to require the protein caveolin. However, as for clathrin-coated domains, the adsorption or insertion of caveolin into a raft domain will modulate the spontaneous curvature, bending rigidity and line tension of this domain, and, thus, may again lead to domain-induced budding.

Even though the existence of rafts is now widely accepted, the structure and size of these rafts is still a matter of controversy. It was concluded from a recent experimental study, in which the diffusion coefficient of anchored proteins was measured by optical methods, that rafts have a size of the order of 20–30 nm [36]. It has also been proposed, however, that the size of rafts may depend on the amount of lateral clustering [37] or crosslinking [38], and that smaller rafts coalesce into larger ones after the preassembly of protein clusters.

The latter process can be understood in terms of the entropy of mixing since the coalescence of larger, preassembled building blocks involves a smaller loss of this entropy. Small raft domains diffusing within a large membrane matrix can again be modelled as in [3] and in Figure 6. The dark patches in this figure now represent small, possibly cross-linked domains which grow into larger domains via coalescence. As soon as these domains have reached their maximal size, they bud and form caveolae.

4. Adhesion-induced Domain Formation

Finally, let us briefly consider a multicomponent membrane which is in contact with another surface, such as a solid substrate or another membrane. One of the intramembrane components is attracted by the second surface and, thus, corresponds to adhesion molecules or local stickers.

There are many different types of stickers which can vary greatly in their size. The smallest stickers are presumably charged head groups of lipids which are attracted towards an oppositely charged surface. Likewise, lipids may have large sticky head groups containing, e.g., polysaccharides. Much larger stickers mediate the specific adhesion of biomembranes which governs both cell-cell adhesion and cell signalling by target cells. The cell adhesion molecules (CAMs), which govern the binding of two cells, are usually relatively stiff rodlike molecules which are anchored in the bilayer membrane and which have a linear extension of 10–30 nm, i.e., large compared to the bilayer thickness.

Adhesion via stickers has been experimentally studied for a variety of multicomponent vesicles [39, 40]. It was observed that these vesicles often have a tendency for domain formation within the contact area. This process is, however, not universal. One system which does not exhibit adhesion-induced phase separation are neurons which adhere to laminin or fibronectin covered silica surfaces [41].

Since the membranes are fluid, the stickers are laterally mobile and the membranes undergo thermally excited shape fluctuations. The behavior of these systems is difficult to predict since it depends on the interplay of several entropic and enthalpic contributions arising from specific sticker-surface and generic surface-surface interactions, lateral sticker-sticker interactions within the same membrane, and shape fluctuations of the membranes.

A systematic study of this interplay shows that these systems exhibit two general cooperative phenomena: (i) In the absence of attractive sticker-sticker interactions, the sticker-mediated adhesion can only occur if the concentration of the stickers exceeds a certain *threshold* value [42]; and (ii) The adhesion via stickers often leads to phase-separation within the membrane, i.e., to the coexistence of sticker-poor and sticker-rich domains [42–46].

Similar phenomena should occur during the adhesion of biomembranes. One interesting possibility is the combination of adhesion-induced domain formation

and domain-induced budding. Such a two-step process could occur after the adhesion of two cells, say *A* and *B*, and could be used by cell *A* to take up membrane segments of cell *B* or vice versa.

References

1. Lipowsky, R.: (a) Budding of membranes induced by intramembrane domains, *J. Phys. II France* **2** (1992), 1825–1840; (b) Domain-induced budding of fluid membranes, *Biophys. J.* **64** (1993), 1133–1138.
2. Jülicher, F. and Lipowsky, R.: (a) Domain-induced budding of vesicles, *Phys. Rev. Lett.* **70** (1993), 2964–2967; (b) Shape transformations of inhomogeneous vesicles with intramembrane domains, *Phys. Rev. E* **53** (1996), 2670–2683.
3. Kumar, S., Gompper, G. and Lipowsky, R.: Budding dynamics of multicomponent membranes, *Phys. Rev. Lett.* **86** (2001), 3911–3914.
4. Döbereiner, H.-G., Käs, J., Noppl, D., Sprenger, I. and Sackmann, E.: Budding and fission of vesicles, *Biophys. J.* **65** (1993), 1396–1403.
5. Bradley, A.J., Maurer-Spurej, E., Brooks, D.E. and Devine, D.V.: Unusual electrostatic effects on binding of C1q to anionic liposomes: Role of anionic phospholipid domains and their line tension, *Biochemistry* **38** (1999), 8112–1823.
6. Holopainen, J.M., Angelova, M.I. and Kinnunen, P.K.J.: Vectorial budding of vesicles by asymmetrical enzymatic formation of ceramide in giant liposomes, *Biophys. J.* **78** (2000), 830–838.
7. Schekman, R. and Orci, L.: Coat proteins and vesicle budding, *Science* **271** (1996), 1526–1533.
8. Simons, K. and Ikonen, E.: Functional rafts in cell membranes, *Nature* **387** (1997), 569–572.
9. Jacobson, K. and Dietrich, C.: Looking at lipid rafts?, *Trends in Cell Biology* **9** (1999), 87–91.
10. Huttner, W.B. and Zimmerberg, J.: Implications of lipid microdomains for membrane curvature, budding and fission, *Curr. Opin. Cell Biol.* **13** (2001), 478–484.
11. Thompson, T.E. and Tillack, T.W.: Organization of glycosphingolipids in bilayers and plasma membranes of mammalian cells, *Ann. Rev. Biophys. Biophys. Chem.* **14** (1985), 361–386.
12. Sek Wen Hui: The spatial distribution of cholesterol in membranes, in: P.L. Yeagle (ed.), *Biology of cholesterol*, CRC Press, Boca Raton, 1988.
13. Scheiffele, P., Rietveld, A., Wilk, T. and Simons, K.: Influenza viruses select ordered lipid domains during budding from the plasma membrane, *J. Biol. Chem.* **274** (1999), 2038–2044.
14. Lu, X. and Silver, J.: Ecotropic murine leukemia virus receptor is physically associated with caveolin and membrane rafts, *Virology* **276** (2000), 251–258.
15. Keller, S.L., Pitcher III, W.H., Huestis, W.H. and McConnell, H.M.: Red blood cell lipids form immiscible liquids, *Phys. Rev. Lett.* **81** (1998), 5019–5022.
16. Dietrich, C., Bagatolli, L.A., Volovyk, Z.N., Thompson, N.L., Levi, M., Jacobson, K. and Gratton, E.: Lipid rafts reconstituted in model membranes, *Biophys. J.* **80** (2001), 1417–1428.
17. Korlach, J., Schwille, P., Webb, W.W. and Feigensohn, G.W.: Characterization of lipid bilayer phases by confocal microscopy and fluorescence correlation spectroscopy, *Proc. Natl. Acad. Sci. USA* **96** (1999), 8461–8466.
18. Bagatolli, L.A. and Gratton, E.: Two-photon fluorescence microscopy observation of shape changes at the phase transition in phospholipid giant unilamellar vesicles, *Biophys. J.* **77** (1999), 2090–2101.
19. Lipowsky, R.: Bending of membranes by anchored polymers, *Europhys. Lett.* **30** (1995), 197–202.
20. Hiergeist, C. and Lipowsky, R.: Elastic properties of polymer-decorated membranes, *J. Phys. France* **6** (1996), 1465–1481.

21. Breidenich, M., Netz, R. and Lipowsky, R.: The shape of polymer-decorated membranes, *Europhys. Lett.* **49** (2000), 431–437.
22. Hiergeist, C., Indrani, V.A. and Lipowsky, R.: Membranes with anchored polymers at the adsorption transition, *Europhys. Lett.* **36** (1996), 491–496.
23. Breidenich, M., Netz, R. and Lipowsky, R.: Adsorption of polymers anchored to membranes, *Eur. Phys. J. E* **5** (2001), 403–414.
24. Decher, G., Kuchinka, E., Ringsdorf, H., Venzmer, J., Bitter-Suermann, D. and Weisgerber, C.: Interaction of amphiphilic polymers with model membranes, *Angew. Makromol. Chem.* **166/167** (1989), 71–80.
25. Simon, J., Kühner, M., Ringsdorf, H. and Sackmann, E.: Polymer-induced shape changes and capping in giant liposomes, *Chem. Phys. Lipids* **76** (1995), 241–258.
26. Döbereiner, H.G., Lehmann, A., Goedel, W., Selchow, O. and Lipowsky, R.: Membrane curvature induced by sugar and polymer solutions, in: B. Mulder, C.F. Schmidt and V. Vogel (eds.), *Materials Science of the Cell* **489**, of *Mat. Res. Soc. Symp. Proc.*, pp. 101–106, MRS, Warrendale, Pennsylvania, 1998.
27. Frette, V., Tsafir, I., Guedeau-Boudeville, M.A., Jullien, L., Kandel, D. and Stavans, J.: Coiling of cylindrical membrane stacks with anchored polymers, *Phys. Rev. Lett.* **83** (1999), 2465–2468.
28. Jakobs, B., Sottmann, T., Strey, R., Allgaier, J., Willner, L. and Richter, D.: Amphiphilic block copolymers as efficiency boosters for microemulsions, *Langmuir* **15** (1999), 6707–6711.
29. Tsafir, I., Guedeau-Boudeville, M.A., Kandel, D. and Stavans, J.: Coiling instability of multilamellar membrane tubes with anchored polymers, *Phys. Rev. E* **63** (2001), 031603/1–11.
30. Gompper, G., Edo, H., Mihailescu, M., Allgaier, J., Monkenbusch, M., Richter, D., Jakobs, B., Sottmann, T. and Strey, R.: Measuring bending rigidity and spatial renormalization in bicontinuous microemulsions, *Europhys. Lett.* (in press).
31. Dimova, R., Döbereiner, H.G. and Lipowsky, R.: In preparation.
32. Lipowsky, R., Döbereiner, H.G., Hiergeist, C. and Indrani, V.: Membrane curvature induced by polymers and colloids, *Physica A* **249** (1998), 536–543.
33. Duwe, H.P., Käs, J. and Sackmann, E.: Bending elastic moduli of lipid bilayers: Modulation by solutes, *J. Phys. France* **51** (1990), 945–962.
34. Benvegnu, D.J. and McConnell, H.M.: Line tension between liquid domains in lipid monolayers, *J. Phys. Chem.* **96** (1992), 6820–6824.
35. Goetz, R., Gompper, G. and Lipowsky, R.: Mobility and elasticity of self-assembled membranes, *Phys. Rev. Lett.* **82** (1999), 221–224.
36. Pralle, A., Keller, P., Florin, E.L., Simons, K. and Hörber, J.K.H.: Sphingolipid-cholesterol rafts diffuse as small entities in the plasma membrane of mammalian cells, *J. Cell Biol.* **148** (2000), 997–1007.
37. Brown, D.A. and London, E.: Structure and origin of ordered lipid domains in biological membranes, *J. Membrane Biol.* **164** (1998), 103–114.
38. Harder, T., Scheiffele, P., Verkade, P. and Simons, K.: Lipid domain structure of the plasma membrane revealed by patching of membrane components, *J. Cell Biol.* **141** (1998), 929–942.
39. Nardi, J., Feder, T., Bruinsma, R. and Sackmann, E.: Electrostatic adhesion between fluid membranes: phase separation and blistering, *Europhys. Lett.* **37** (1997), 371–376.
40. Albersdörfer, A., Feder, T. and Sackmann, E.: Adhesion-induced domain formation by interplay of long-range repulsion and short-range attraction force: A model membrane study, *Biophys. J.* **73** (1997), 245–257.
41. Braun, D. and Fromherz, P.: Fluorescence interferometry of neuronal cell adhesion on microstructured silicon, *Phys. Rev. Lett.* **81** (1998), 5241–5244.
42. Lipowsky, R.: Adhesion of membranes via anchored stickers, *Phys. Rev. Lett.* **77** (1996), 1652–1655.

43. Weikl, T., Netz, R. and Lipowsky, R.: Unbinding transitions and phase separation of multi-component membranes, *Phys. Rev. E* **62** (2000), R45–R48.
44. Bruinsma, R., Behrisch, A. and Sackmann, E.: Adhesive switching of membranes: Experiment and theory, *Phys. Rev. E* **61** (2000), 4253–4267.
45. Komura, S. and Andelman, D.: Adhesion-induced lateral phase separation in membranes, *Eur. Phys. J. E* **3** (2000), 259–271.
46. Weikl, T. and Lipowsky, R.: Adhesion-induced phase behavior of multicomponent membranes, *Phys. Rev. E* **64** (2001), 11903–11915.